ELSEVIER

Chemical Physics 267 (2001) 161–171

Chemical Physics

www.elsevier.nl/locate/chemphys

# Coherent control of second harmonic generation using spectrally phase coded femtosecond waveforms

Z. Zheng *, A.M. Weiner

*School of Electrical and Computer Engineering, Purdue University, 1285 EE Building, P.O. Box 543, West Lafayette, IN 47907-1285, USA*

Received 31 August 2000

**Abstract**

We report the demonstration of coherent control of second harmonic generation (SHG) with over three orders of magnitude contrast in the SHG yield. Under conditions of large group-velocity mismatch and narrow phase matching bandwidth, we show that SHG can serve (in the perturbative limit) as a nonlinear optical but classical analogue for quantum mechanical two-photon transitions in atomic media, with advantages in efficiency and ease of implementation. Our coherent control scheme results in a spectral phase correlator for ultrashort pulse waveforms, which may have applications in novel high-bandwidth optical communication schemes. We demonstrate a set of different waveforms with similar strong control yields by introducing families of binary phase codes taken from communication theory into the coherent control process. The response to these waveforms under certain nonideal situations is also studied. © 2001 Published by Elsevier Science B.V.

*PACS:* 42.65.Ky; 42.65.Re; 42.79.Sz; 32.80.Qk
*Keywords:* Coherent control; Second harmonic generation; Optical pulse shaping; Ultrafast optics; Nonlinear optics

## 1. Introduction

The recognition of the coherence of quantum mechanical processes had led to attempts of actively manipulating various quantum systems using coherent laser excitation [1]. These laser techniques are based on either the manipulation of multiple interfering pathways [2–4] or the use of specially shaped ultrafast optical waveforms [5–10] synthesized through femtosecond pulse shaping methods [11–17], and a number of intriguing experimental results on coherent manipulation of molecules and atoms have been reported. Here we demonstrate coherent control of second harmonic generation (SHG) with over three orders of magnitude contrast in the SHG yield [18]. We study SHG under conditions of large group-velocity mismatch (GVM) [19,20], which leads to a sharp resonance in the SHG spectrum due to the phase matching condition for the nonlinear conversion process. This allows SHG to serve (in the perturbative limit) as a nonlinear optical but classical analogue for quantum mechanical two-photon processes which have previously been studied [10]. Our scheme blends elements of both the multiple pathways and the shaped short pulse control schemes, which are usually considered separately

* Corresponding author. Tel.: +1-765-494-3394; fax: +1-765-494-6951.
*E-mail address:* zzheng@ecn.purdue.edu (Z. Zheng).

0301-0104/01/$ - see front matter © 2001 Published by Elsevier Science B.V.
PII: S0301-0104(01)00220-8

in coherent control experiments. We introduce the use of families of binary phase codes taken from communication theory into the coherent control process, which allows us to demonstrate a whole family of different waveforms with similar control yields. An important motivation for our work is that the coherent control relationship between the SHG yield and the form of the phase coded femtosecond waveform may provide a mechanism for recognizing specially shaped femtosecond pulses in a proposed ultrafast optical code-division multiple access fiber optic communication system [21–23]. To our knowledge, this may be the first example of an application of coherent control concepts to optical communications!

SHG is one of the oldest nonlinear optical phenomena studied [24], where the pump (fundamental) optical wave of frequency $\omega$ propagating in dielectric material is converted to a wave at $2\omega$ due to the nonlinear polarization of the media. Efficient SHG is only possible when the phase velocities of the fundamental and second harmonic (SH) waves are matched so that the generated SH signals can constructively build up in the process. However, because of the existence of phase velocity dispersion, the phase matching condition between the interacting waves is often not met, and the SHG efficiency is severely limited. In order to compensate this phase velocity dispersion, traditionally phase matching techniques based on material birefringence are needed to achieve efficient nonlinear interactions. More recently, quasi-phase-matching (QPM) techniques [25,26] are under intensive studies, which achieve high SHG conversion efficiency by periodically modulating the material nonlinear coefficient to offset the accumulated material phase mismatch.

The situation is more complicated when ultrashort optical pulses are used in the SHG process. Because of the broad bandwidth of the pump light, the SH signals may have broad spectra which can support complex structures. Each SH spectral component results from the coherent addition of different pairs of the frequency components at the fundamental frequency, similar to the final quantum state of a quantum mechanical transition that is the superposition of excitations from various 'pathways'. In addition, the high peak intensity of the excitation pulses enhances the efficiency of the nonlinear frequency conversion process, leading to the possibility of very high efficiency.

When short pulses are used, the GVM effect can also affect the SHG spectral bandwidth. In the dispersive medium, since the pump pulse and the SH pulse are at different wavelengths, their group velocities are different. This GVM causes the two pulses to gradually walk off from each other in the time domain. As illustrated in Fig. 1, when thin nonlinear crystals (NLCs) are used, the walk-off effect is small, so that the two pulses can stay together in the SHG process and a short SH pulse is generated, which has a broad spectrum. On the other hand, for thick crystals, the pump pulse and the generated SH pulse significantly walk off from each other when they propagate through the crystal, so that the generated SH pulse can be much longer than the pump pulse, and its spectrum is narrowed correspondingly.

For a sufficiently thick crystal with sufficiently strong spectral narrowing, there is essentially only a single SH frequency available for the SHG process. We demonstrate here that the SHG yield can be manipulated very strongly under this thick crystal condition by modulating the relative phases between the coherent pump frequencies so that the generated SHG signals by different 'pathways' can add up either constructively or destructively. Although SHG does not require a quantum mechanical description, there is a close analogy between SHG under large GVM conditions and two photon absorption (TPA) to a single resonant quantum state (see Fig. 2). Therefore, our control scheme is in close relationship with those used with these quantum mechanical systems such as in Ref. [10].

Our study may also be applied to a multi-access optical communication scheme based on spectral phase coding of ultrashort pulses [21,22]. In such a network (Fig. 3), ultrashort pulses are coded at the transmitter with a spectral phase code $C_1$ by the encoder (e.g. a pulse shaper) and the coded signals are transmitted along with signals encoded with other codes from other users. At the receiver side, a second spectral code $C_2$ is applied by the decoder. If $C_2$ properly matches $C_1$, the signal can be decoded. Otherwise, the signal should be rejected

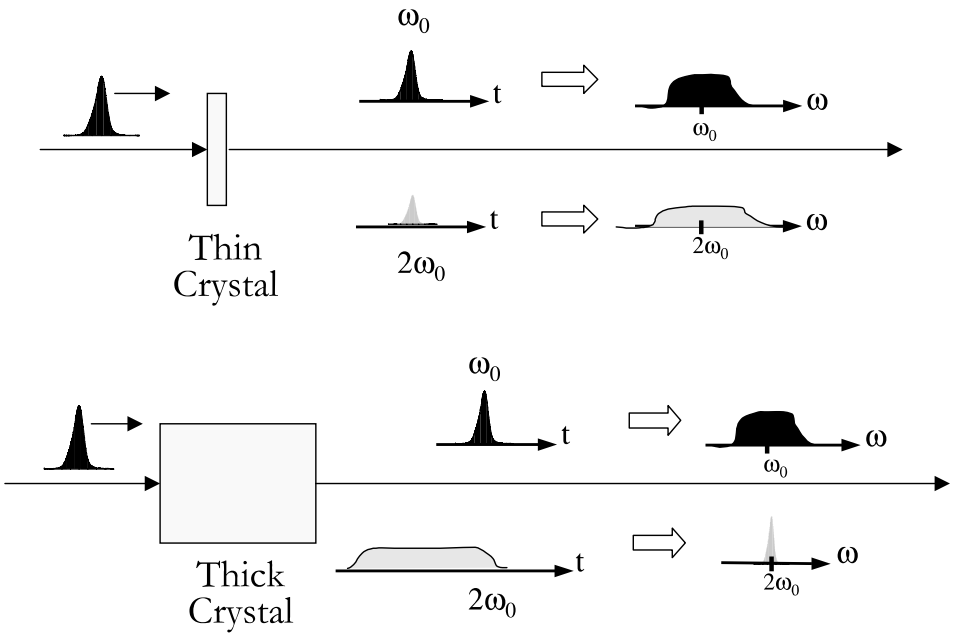


Fig. 1. Illustration of SHG in thin crystals and thick crystals.

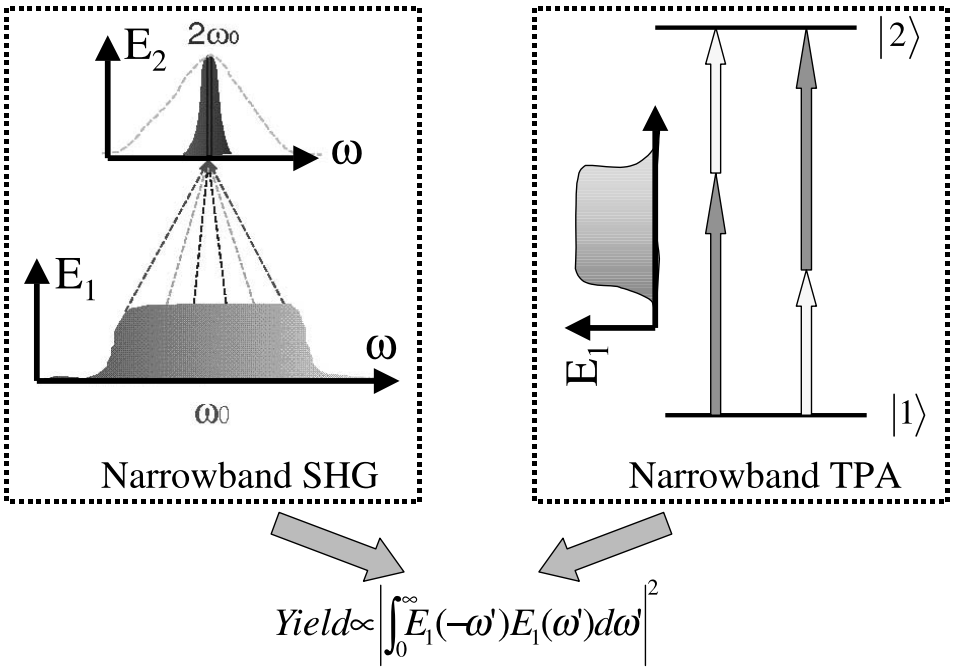


Fig. 2. Narrow bandwidth SHG and narrowband TPA.

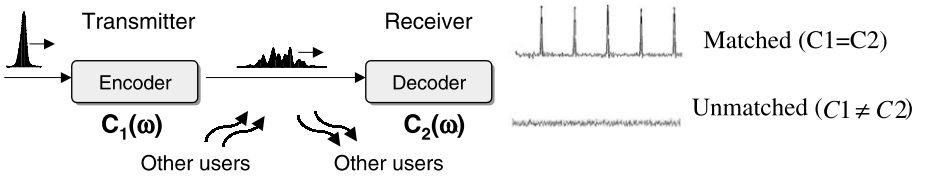


Fig. 3. Illustration of fiber optical communication systems based on spectral phase coding of ultrashort pulses.

and ignored by the receiver. As we will show later, our coherent control scheme may serve as an optical spectral correlator to recognize waveforms based on the spectral phase codes applied. Such waveform recognition schemes may represent a new opportunity for coherent control concepts to impact high-speed communication and information processing.

## 2. Theoretical analysis

Mathematically, under the slowly varying envelope approximation, the small-signal condition and the type-I phase matching condition [19], the evolution of the SH spectrum envelope function $A_2$ is described by

$$\frac{\mathrm{d}}{\mathrm{d}z}A_2(z,\Omega) = -\mathrm{i}\frac{\mu_0\omega^2}{2k_2(\Omega)}\widehat{P_{\mathrm{NL}}}(z,\Omega)\exp(\mathrm{j}k_2(\Omega)z), \tag{1}$$

where the nonlinear polarization spectrum $\widehat{P_{\mathrm{NL}}}$ is the Fourier transform of the nonlinear polarization $P_{\mathrm{NL}} = \epsilon_0 \mathrm{d}(z)E_1^2(z,t)$. Here $\Omega$ is the detuning of the angular frequency from the spectral center angular frequency of the SH wave, $\mathrm{d}(z)$ is the position-dependent nonlinear coefficient, $k_2(\Omega)$ is the amplitude of the wave vector for the SH wave.

By integrating Eq. (1) over $z$, we get the output $A_2$:

$$\begin{aligned} A_2(\Omega) = &\int_{-\infty}^{\infty}\mathrm{d}z'\Gamma(z')\exp(\mathrm{j}k_2(\Omega)z') \\ &\times\int_{-\infty}^{\infty}A_1(\Omega')A_1(\Omega-\Omega') \\ &\times\exp(-\mathrm{j}[k_1(\Omega')+k_1(\Omega-\Omega')]z)\,\mathrm{d}\Omega', \end{aligned} \tag{2}$$

where $\Gamma(z) = -\mathrm{j}2\pi\mathrm{d}(z)/\lambda_1 n_2$ is the nonlinear coupling coefficient, and $A_1$ and $k_1$ are the Fourier transform of the field envelope function and the amplitude of the wave vector of the fundamental wave. Here $\lambda_1$ is the fundamental wavelength and $n_2$ is the refractive index at the pump wavelength.

For a uniform NLC of length $L$, when the intrapulse group velocity dispersion (GVD) is negligible and the fundamental and SH waves are phase matched at the center frequency of their spectrum, Eq. (2) can be simplified to [26]:

$$\begin{aligned} A_2(\Omega) &= 2\int_0^{\infty}A_1(\Omega/2+\Omega')A_1(\Omega/2-\Omega')\,\mathrm{d}\Omega' D(\Omega) \\ &= 2\int_0^{\infty}A_1(\Omega/2+\Omega')A_1(\Omega/2-\Omega')\,\mathrm{d}\Omega' \\ &\quad\times\Gamma L\,\mathrm{sinc}(\Omega\alpha L/2), \end{aligned} \tag{3}$$

where $\alpha = 1/v_{\mathrm{g},1} - 1/v_{\mathrm{g},2}$ is the GVM between the fundamental pulse and the SH pulse, as $v_{\mathrm{g}}$ is the group velocity and $\partial k/\partial\omega = v_{\mathrm{g}}^{-1}$. The transfer function $D(\Omega)$ and second term on the RHS of the equation represent the effect of phase matching condition on the SHG spectrum generated, and Eq. (3) shows that group velocity mismatch imposes a fundamental limit on the SH bandwidth that may be obtained via the nonlinear frequency conversion process.

### 2.1. Thin nonlinear crystals and broadband SHG

When thin NLCs (i.e., $L \ll \tau/|\alpha|$, where $\tau$ is the pulsewidth of an unchirped pump pulse) are used, the temporal walk off between the fundamental and SH pulses is small compared to their pulsewidths, so that the two pulses stay together in the nonlinear interaction process. In this limit, the function $D(\Omega)$ is much broader than the source

term (the auto-convolution term of $A_1$) on the right hand side of Eq. (3), and it can be considered as constant in the region of interest and its effect can be ignored. For broadband SHG, the SHG power $P_{\mathrm{SHG}}$ is given by

$$\int_{-\infty}^{\infty}\left|\int_{-\infty}^{\infty}A_1(\Omega/2+\Omega')A_1(\Omega/2-\Omega')\,\mathrm{d}\Omega'\right|^2\mathrm{d}\Omega = \int_{-\infty}^{\infty}I_1^2(t)\,\mathrm{d}t, \tag{4}$$

where $I_1$ is the temporal intensity function of the pump pulse. Therefore, the SHG power is only related to the optical intensity and not sensitive to the optical temporal phase distributions. It is noted that the TPA into continuum can also be described by an equation in the same form of Eq. (4) [23].

### 2.2. Thick nonlinear crystals and narrowband SHG

On the other hand, in thick crystals, where the GVM is large (i.e. $L \gg \tau/|\alpha|$), $D(\Omega)$ can be significantly narrower than the first term on the right hand side of Eq. (3). This limits the possible SHG frequency bandwidth to $\sim 0.88/(L|\alpha|)$ [19]. In applications where broadband SHG is required, which include most femtosecond applications, this spectral narrowing effect is considered unfavorable and, therefore, left largely unexplored. Equivalently in the time domain, the GVM between fundamental and SH pulses causes the SH pulses to walk off from the fundamental, which leads to a temporal broadening of the SH output pulse. This is also usually considered undesirable, and therefore most femtosecond experiments are performed with thin SHG crystals ($L \ll \tau/|\alpha|$).

However we show that in a coherent control context, the GVM can be beneficial. Consider the situation where the length of the NLC is very large, so that $D(\Omega)$ approaches a $\delta$-function. Then the output SHG power is given as [18]

$$\int_{-\infty}^{\infty}|A_2(\Omega)|^2\,\mathrm{d}\Omega = 8\pi\Gamma^2 L\left|\int_0^{\infty}A_1(\Omega')A_1(-\Omega')\,\mathrm{d}\Omega'\right|^2\Big/|\alpha|, \tag{5}$$

i.e. it is proportional to the self-convolution of the pump field spectrum. As it is related to the field instead of intensity functions, this is sensitive to the phase functions and is fundamentally different from the broadband two-photon processes, like SHG in thin crystals or TPA into a continuum [23]. It should be noted that the transition probability for TPA in an atomic medium (i.e. with narrow discrete initial and final states) has the same functional form as the above equation, assuming the weak response condition and no intermediate resonance [27], as shown in Fig. 2. This has formed the basis for experiments on coherent quantum control of two photon transitions using pulses shaped via a sinusoidal spectral phase modulation [10]. Therefore, our experiments can be regarded as a nonlinear optical but completely classical analogue for the weak field quantum control experiments observed in Ref. [10].

Eq. (5) also shows that the SH power scales linearly with $L$. For large $L$ ($\sim$cm), highly efficient SHG of femtosecond pulses can be achieved even under conditions of large GVM. This was demonstrated in Ref. [28], where nearly 60% SHG conversion efficiency was obtained using only $\sim$150 mW average power from a modelocked Ti:sapphire laser oscillator. This potential for high efficiency relative to the quantum systems studied in most coherent control schemes is of significant importance in applications where the power budget is very stringent, e.g., high speed communication systems.

## 3. Control scheme

Based on Eq. (5) above, we design our optical waveforms for the coherent control of SHG under the large GVM condition in the following way, as illustrated in Fig. 4: our input spectrum has a flat-top (e.g. $|A_1(\Omega')|$ is constant within a certain frequency range and zero otherwise) and unchirped. The fundamental spectrum is divided into $2N$ 'channels' with an equal frequency width, each of which is given a phase shift $\Phi_i$ ($i = -N,\ldots,-1,1,\ldots,N$). We divide the spectrum in half and call the phase patterns on the low

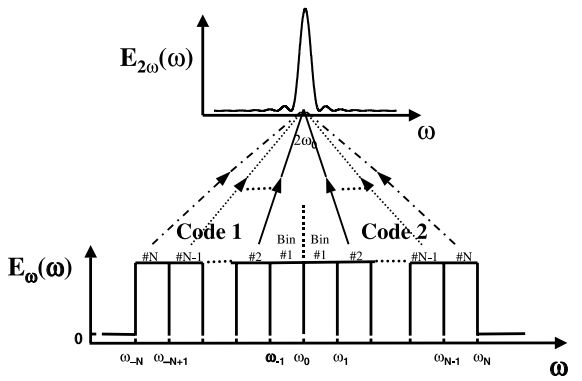


Fig. 4. Scheme of optical phase coding for the control of SHG by ultrashort pulses.

frequency and high frequency sides of the spectrum $C_1 = \{\Phi_{-1} \cdots \Phi_{-N}\}$ and $C_2 = \{\Phi_1 \cdots \Phi_N\}$, respectively. Thus the SHG signal would be the coherent sum of the signals from $N$ pairs of channels and is proportional to

$$\left| \sum_{i=1}^{N} \exp(j\Phi_i) \exp(j\Phi_{-i}) \right|^2, \tag{6}$$

e.g. the square of the magnitude of the correlation function between code words $C_1$ and $C_2$. The SHG yield can then be manipulated by changing the correlation properties of the applied spectral phase functions. This provides the opportunity for coherent control.

In the fiber optical communication scenario, the spectral phase code $C_1$ is applied at the transmitter to the spectrum and $C_2$ is applied by the receiver. Based on our previous discussion, we know that SHG in long NLCs can work as an optical spectral correlator. If the $C_1$ and $C_2$ are selected from a code set with low cross correlations, only the signals coded with a matched $C_1$ and $C_2$ pair can generate significant SHG output, and the pulses coded with unmatched $C_1$ and $C_2$ will generate little signal. Thus the rejection of multi-access interference noise is realized.

It should be noted that for NLCs with a spatially nonuniform or modulated nonlinearity, the $D(\Omega)$ can be engineered to have various shapes other than the simple sinc function in Eq. (3) [26,29]. This raises the possibility of generating multiply peaked resonances, which could serve as a nonlinear optical, classical analogue for multi-level atoms in future experiments.

## 4. Experimental setup

Our experimental setup is shown in Fig. 5. 120 fs pulses from a stretched-pulse modelocked fiber laser [30] were delivered to a fiber-pigtailed femtosecond pulse shaper [22]. In the pulse shaper, the spectral components of the input pulse are spatially dispersed by a grating-lens pair, manipulated by using a spatial light modulator, and then recombined into a collimated beam by using a second lens-grating pair. The temporal profile of the waveform after the pulse shaper is determined by the Fourier transform of the pattern imposed onto the spectrum. For these experiments we used a computer controlled, 128 pixel programmable amplitude/phase liquid crystal modulator (LCM) array [12,16], which allows each pixel of the array to be individually programmed for independent gray-scale amplitude and phase modulation. The output pulses from the pulse shaper had an energy of ~2 pJ, and a spectrum ~18 nm wide centered at ~1559.5 nm. After transmission by an ~4 m length of single mode fiber, the pulses were coupled into free space and then loosely focused into a periodically poled lithium niobate (PPLN) crystal, with a depth of focus chosen to be longer than the crystal. The polarization was controlled by a half-wave plate so that the light was polarized along the $z$-axis of the crystal. PPLN, which has been the most intensively studied nonlinear frequency conversion crystal in the past few years, is ideal for our application because of its high nonlinearity for frequency doubling at our wavelength, large GVM parameter (0.3 ps/mm), noncritical phase matching which avoids spatial walk off, and availability in relatively large sizes [25]. We used a commercial PPLN crystal which was 20 mm long and 0.5 mm thick and had a QPM grating with 19.0 μm period. The crystal was heated to a temperature of ~100°C so that the center of the input spectrum was phase matched and the photorefractive effect was eliminated. The SHG output at 0.78 μm

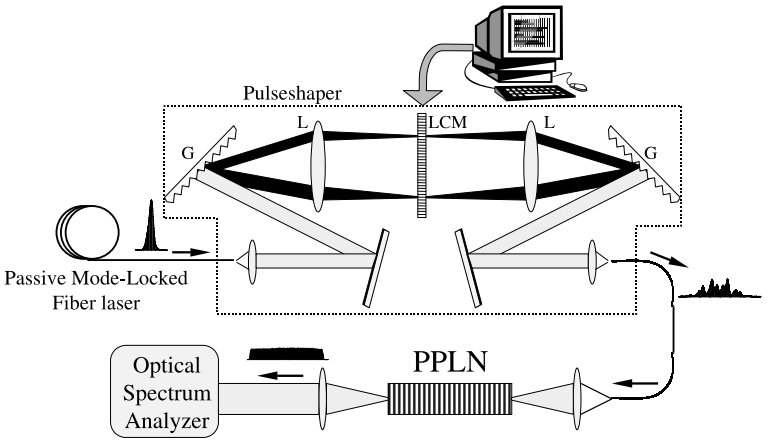


Fig. 5. Scheme of experimental setup. The system consisted of a passively mode-locked laser, a femtosecond fiber-pigtailed pulseshaper, a piece of PPLN placed in a temperature controlled oven and a spectrometer. The pulseshaper consisted of a pair of 1100 lines/mm gratings and achromatic lenses (focal length = 19 cm) and an amplitude/phase LCM.

wavelength generated by the PPLN was collected and sent into a computer controlled spectrometer with a resolution of ~0.03 nm. A photomultiplier tube and lock-in amplifier were used in the detection system. The SHG spectra were measured as various phase code pairs of $C_1$ and $C_2$ were imposed on the pump pulses.

## 5. Experimental results

Before generating coded waveforms, we programmed the pulse shaper in order to satisfy the assumptions of a flat and unchirped spectrum. The input spectrum amplitude was equalized by applying a transmittance function to the LCM which was proportional to the inverse of the original optical power spectrum, as measured by an optical spectrum analyzer in the 1.5 μm wavelength band. The pump spectrum before and after gain equalization is shown in Fig. 6. The residual phase chirp from the fiber system was also compensated by programming the pulse shaper for an equal and opposite spectral phase, similar to experiments in which programmable pulse shapers have been used to compensate for residual chirps in fiber transmission systems [31] and high power chirped pulse femtosecond amplifiers [32].

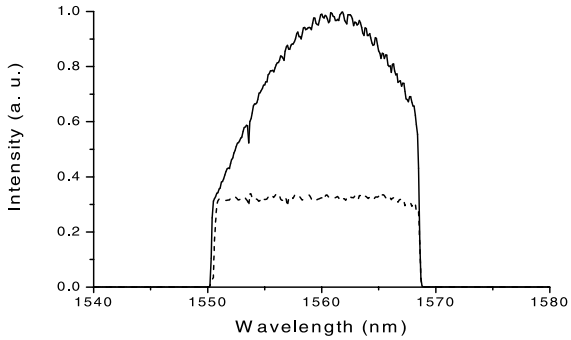


Fig. 6. Gain equalization of the pump spectrum.

Here we used Hadamard codes to construct our spectral phase functions. Hadamard codes have been widely studied and applied in communications and signal processing [33,34]. Linear Hadamard code sets exist for the code length of $m = 2^n$, where $n$ is an positive integer and greater than 1. For the codewords of the same length $2^n$, they are obtained by choosing the row vectors of a $m \times m$ Hadamard matrix and, therefore, there are $m$ Hadamard codewords of the length $m$. These codewords are also orthogonal to each other in their bipolar form. Each codeword consists of $m/2$ ones and $m/2$ minus ones.

Here we used eight different length-8 phase codes from an $8 \times 8$ Hadamard matrix:

$$\begin{bmatrix} -1 & -1 & -1 & -1 & -1 & -1 & -1 & -1 \\ -1 & 1 & -1 & 1 & -1 & 1 & -1 & 1 \\ -1 & -1 & 1 & 1 & -1 & -1 & 1 & 1 \\ -1 & 1 & 1 & -1 & -1 & 1 & 1 & -1 \\ -1 & -1 & -1 & -1 & 1 & 1 & 1 & 1 \\ -1 & 1 & -1 & 1 & 1 & -1 & 1 & -1 \\ -1 & -1 & 1 & 1 & 1 & 1 & -1 & -1 \\ -1 & 1 & 1 & -1 & 1 & -1 & -1 & 1 \end{bmatrix}. \quad (7)$$

To convert the binary codes to phase codes, we set $\Phi_i$ to $\pi$ when the corresponding code bit is $-1$, and to 0 when the corresponding bit is 1. In the following experiments, $C_1$ was set to be the second code word $[-1\ 1\ -1\ 1\ -1\ 1\ -1\ 1]$ in the Hadamard code set (see Eq. (7)), while $C_2$ is varied among the eight words in the set. The concatenated codes therefore had the length of 16. Each code bit has a bandwidth in the spectral domain of about 1.1 nm and corresponds on average to eight pixels in the LCM. The overall modulation function applied by the LCM was the superposition of the amplitude equalization function, the chirp compensation function and the phase coding functions.

The spectral phase coding process spreads the unchirped femtosecond input pulse into lower intensity waveforms approximately 10 ps long and with complicated substructures, as shown in Fig. 7. For different choices of $C_2$, the intensity profiles look quite similar, while the phase substructure and the correlation properties of the concatenated codes and thus the expected control yield are quite different. For the case of a code of highly correlated code words (in this case the same word, $C_1 = C_2$), the waveform is not expected to be chirped in the time domain, and comparable SHG yield as the uncoded pulse case is expected even though the peak intensity of the waveform had been significantly reduced. For other cases where the spectrum consists of two orthogonal code words ($C_1 \neq C_2$), the corresponding waveform is expected to have a nonuniform temporal phase distribution, and only little SHG signal is expected.

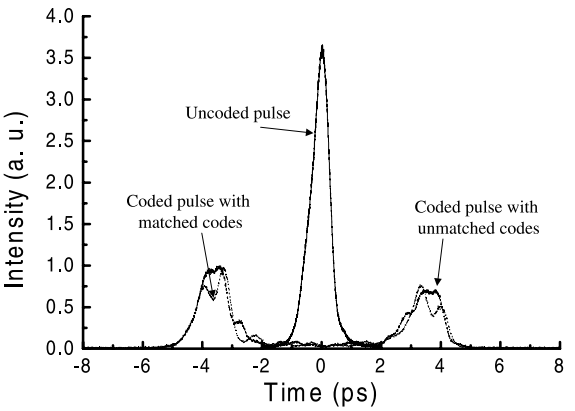


Fig. 7. Pulse shapes of uncoded pulse, coded pulse with matched codes and coded pulse with unmatched codes.

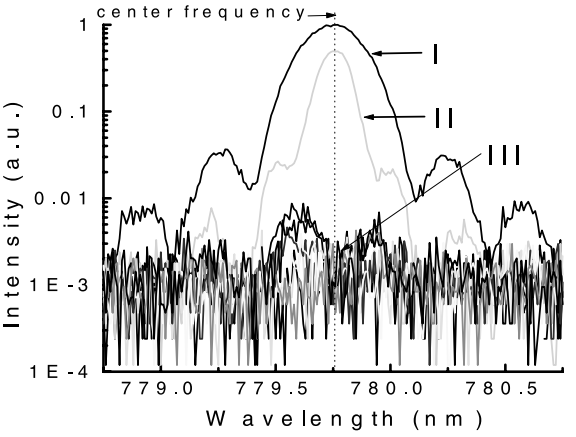


Fig. 8. SHG spectra measured under different spectral phase coding situations. $C_1$ in the phase codes is set to $\{-1\ 1\ -1\ 1\ -1\ 1\ -1\ 1\}$, the second code word in the Hadamard matrix (Eq. (7)). $C_2$ in the phase codes is set to all the code words in the set. I – no phase code was applied to the pump pulses, II – the phase code used was matched and symmetric to the center, III – other phase codes were applied.

The SHG spectra measured for different choices of $C_2$ are plotted in Fig. 8. Also shown is the SHG spectrum when no phase code was used. In that case, the SHG generated from the equalized, unchirped pump input has a $\text{sinc}^2$ shape with a bandwidth of $\sim$0.3 nm, in good agreement with the result from Eq. (3) and much narrower than the 18 nm input spectrum. This shows the uniformity of the PPLN and the temperature distri-

bution in the crystal. For coded pulses, the seven traces corresponding to $C_1 \neq C_2$ show very weak SHG, especially at the center of the SHG spectrum (779.75 nm), due to the orthogonality of the Hadamard codes, as predicted by theory. Compared with the peak of the uncoded pulses, the signals were always suppressed by a factor of at least 600 and sometimes above 1500 (limited by the noise floor of our measurements). In the situation with correlated codes ($C_1 = C_2$, as in curve II), strong SHG was observed. The SHG peak is comparable to that of the uncoded case (curve I), even though the input pulse has been dispersed significantly in time. The SHG bandwidth is now dominated by the correlation function of the code and is narrower than in curve I. Theoretically it is predicted that the SHG signal should have a sharp peak with the same peak height as the uncoded case. Small imperfections in the coding process and in the control of the input pulse as well as the limited spectral resolution of the spectrometer are responsible for the small differences in the peak intensities of curves I and II. These effects also contribute to the very small but nonzero SHG at the center frequency in the seven unmatched cases. In general, our results are in excellent agreement with the theory.

We note that, in addition to length-8 Hadamard codes, there are other types of orthogonal codes and other code lengths. Therefore, many other optical waveforms are possible which, under ideal conditions, should have very similar SHG control yields. Therefore, our scheme opens up a large set of possible optical waveforms to realize a specific control goal generated with optical phase modulations more complicated than simple symmetric or antisymmetric functions.

Even though the optical waveforms used to realize a specific coherent control goal can be carefully designed beforehand, in reality, the often inevitable nonideal realization of the scheme can adversely affect the eventual outcome. One of the most common nonideal experimental conditions for ultrafast optical systems is dispersion. In Fig. 9, we show the SHG spectra of the coded pump waveforms with the existence of a quadratic spectral distortion (~0.018 ps/nm), which can be caused by residual second-order dispersion in the

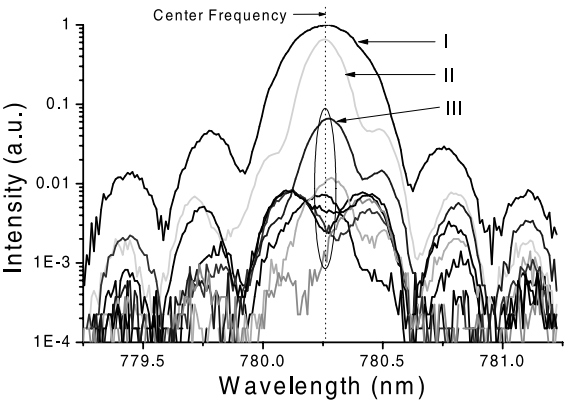


Fig. 9. SHG spectra measured under different spectral phase coding situations with the existence of quadratic spectral phase distortion, I – no phase code was applied to the pump pulses, II – the phase code used was matched and symmetric to the center, III – other phase codes were applied.

laser system or in our case by the fiber leads. This set of waveforms which showed very similar SHG suppression in Fig. 8 under chirp-free conditions now show quite different results. Not only are the shapes of the SHG spectra different, but some codes now generate much more SHG than others. This difference lies in the different symmetry of the spectral codes used and implies that some code combinations may be more 'vulnerable' to chirps than others. With a large number of different spectral codes available to us based on our coherent control scheme, it may be possible to select some of them which are less susceptible to experimental nonideal situations.

However, we have observed that third-order dispersion, which also often plays an important role for ultrashort pulse systems, has nearly no effect on the control yields in our scheme. This finding can be easily explained by the following equation. The yield of coded pump pulses with the third-order dispersion represented by a cubic spectral phase term is proportional to

$$\left|\sum_{i=1}^{N} \exp(\mathrm{j}(\Phi_i + a\Omega^3)) \exp(\mathrm{j}(\Phi_{-i} - a\Omega^3))\right|^2 = \left|\sum_{i=1}^{N} \exp(\mathrm{j}\Phi_i) \exp(\mathrm{j}\Phi_{-i})\right|^2. \quad (8)$$

Here $a$ represents the strength of the third-order dispersion, and the antisymmetric phase distortions on the two sides cancel each other out. This 'invulnerability' to odd-order dispersions could be helpful for systems where pulses with pulsewidth of tens of femtoseconds or shorter are used and third-order dispersion is unavoidable and often difficult to control. This insensitivity to third-order dispersion is also important for the fiber communications application, where cubic spectral phase is often the limiting factor for ultrashort pulse transmission [22,31,35].

## 6. Conclusions

In summary, we have demonstrated high contrast coherent control in femtosecond SHG by specially designed femtosecond optical waveforms. This work demonstrates that a nonlinear optical but completely classical system can serve as an analogue for the two-photon quantum processes studied in the low intensity regime in several previous coherent control experiments [9,10]. Furthermore, we have shown that the use of orthogonal codes makes a large set of waveforms available to realize the same control objective. Our experiments also suggest the possibility of using coherent control concepts for information processing in an optical communications context [21,22]. Finally, taking advantage of recent advances in material fabrication techniques, we can anticipate further significant improvements in the sensitivity and conversion efficiency by using PPLN nonlinear optical waveguides [36] due to the significant increase in the optical intensities of the tightly confined optical beams in the waveguide structure, as well as the ability to design the SHG response to emulate more complicated quantum systems using patterned (aperiodically poled) quasi-phase-matched SHG crystals. We have recently demonstrated more than two order of magnitude SHG efficiency increase by using PPLN waveguides [37], where the results suggest that the optical spectral code correlator could operate at a power level as low as 0.1 pJ per pulse for real-time pulse processing for $\sim$10 Gb/s communication applications. These 'emulators' which are very sensitive and easy to implement could be used to test and optimize the optical waveforms for other coherent control schemes.

## Acknowledgements

This work was supported by the National Science Foundation under 9900369-ECS. We gratefully acknowledge Shuai Shen for use of the femtosecond fiber laser.

## References

[1] H. Rabitz, R. de Vivie-Riedle, M. Motzkus, K. Kompa, Science 288 (5467) (2000) 824–828.
[2] C. Chen, Y.Y. Yin, D.S. Elliott, Phys. Rev. Lett. 64 (5) (1990) 507–510.
[3] A. Shnitman, I. Sofer, I. Golub, A. Yogev, M. Shapiro, Z. Chen, P. Brumer, Phys. Rev. Lett. 76 (16) (1996) 2886–2889.
[4] L.C. Zhu, V. Kleiman, X.N. Li, S.P. Lu, K. Trentelman, R.J. Gordon, Science 270 (5233) (1995) 77–80.
[5] A.M. Weiner, D.E. Leaird, G.P. Wiederrecht, K.A. Nelson, Science 247 (4948) (1990) 1317–1319.
[6] A. Assion, T. Baumert, M. Bergt, T. Brixner, B. Kiefer, V. Seyfried, M. Strehle, G. Gerber, Science 282 (5390) (1998) 919–922.
[7] C.J. Bardeen, V.V. Yakovlev, K.R. Wilson, S.D. Carpenter, P.M. Weber, W.S. Warren, Chem. Phys. Lett. 280 (1–2) (1997) 151–158.
[8] T.C. Weinacht, J. Ahn, P.H. Bucksbaum, Nature 397 (6716) (1999) 233–235.
[9] B. Broers, L.D. Noordam, H.B. van Linden van den Heuvell, Phys. Rev. A 46 (5) (1992) 2749–2756.
[10] D. Meshulach, Y. Silberberg, Nature 396 (6708) (1998) 239–242.
[11] A.M. Weiner, J.P. Heritage, E.M. Kirschner, J. Opt. Soc. Am. B 5 (8) (1988) 1563–1572.
[12] A.M. Weiner, D.E. Leaird, J.S. Patel, J.R. Wullert II, IEEE J. Quant. Electron. 28 (4) (1992) 908–920.
[13] A.M. Weiner, Prog. Quant. Electron. 19 (3) (1995) 161–237.
[14] D. Meshulach, D. Yelin, Y. Silberberg, Opt. Commun. 138 (4–6) (1997) 345–348.
[15] A.M. Weiner, Rev. Sci. Instrum. 71 (5) (2000) 1929–1960.
[16] M.M. Wefers, K.A. Nelson, Opt. Lett. 20 (9) (1995) 1047–1049.
[17] M.A. Dugan, J.X. Tull, W.S. Warren, J. Opt. Soc. Am. B 14 (9) (1997) 2348–2358.
[18] Z. Zheng, A.M. Weiner, Opt. Lett. 25 (13) (2000) 984–986.
[19] W.H. Glenn, IEEE J. Quant Electron. QE-5 (6) (1969) 284–290.

[20] A.M. Weiner, IEEE J. Quant. Electron. 19 (8) (1983) 1276–1283.
[21] J.A. Salehi, A.M. Weiner, J.P. Heritage, J. Lightwave Tech. 8 (3) (1990) 478–491.
[22] H.P. Sardesai, C.C. Chang, A.M. Weiner, J. Lightwave Tech. 16 (11) (1998) 1953–1964.
[23] Z. Zheng, S. Shen, H. Sardesai, C.C. Chang, J.H. Marsh, M.M. Karkhanehchi, A.M. Weiner, Opt. Commun. 167 (1999) 225–233.
[24] P.A. Franken, A.E. Hill, C.W. Peters, G. Weinreich, Phys. Rev. Lett. 7 (1961) 118–119.
[25] L.E. Myers, R.C. Eckardt, M.M. Fejer, R.L. Byer, W.R. Bosenberg, J.W. Pierce, J. Opt. Soc. Am. B 12 (11) (1995) 2102–2115.
[26] G. Imeshev, M.A. Arbore, M.M. Fejer, A. Galvanauskas, M. Fermann, D. Harter, J. Opt. Soc. Am. B 17 (2) (2000) 304–318.
[27] D. Meshulach, Y. Silberberg, Phys. Rev. A 60 (2) (1999) 1287–1292.
[28] A.M. Weiner, A.M. Kan'an, D.E. Leaird, Opt. Lett. 23 (18) (1998) 1441–1443.
[29] G. Imeshev, A. Galvanauskas, D. Harter, M.A. Arbore, M. Proctor, M.M. Fejer, Opt. Lett. 23 (11) (1988) 864–866.
[30] K. Tamura, H.A. Haus, E.P. Ippen, Electron. Lett. 28 (24) (1992) 2226–2228.
[31] C.C. Chang, H.P. Sardesai, A.M. Weiner, Opt. Lett. 23 (4) (1998) 283–285.
[32] A. Sullivan, W.E. White, Opt. Lett. 20 (2) (1995) 192–194.
[33] M. Kavehrad, D. Zaccarin, J. Lightwave Tech. 13 (3) (1995) 534–545.
[34] M. Harwit, N.J.A. Sloane, Hadamard Transform Optics, Academic Press, New York, 1979.
[35] S. Shen, A.M. Weiner, IEEE Photon. Technol. Lett. 11 (7) (1999) 827–829.
[36] A. Galvanauskas, K.K. Wong, K. El Hadi, M. Hofer, M.E. Fermann, D. Harter, M.H. Chou, M.M. Fejer, Electron. Lett. 35 (9) (1999) 731–733.
[37] Z. Zheng, A.M. Weiner, K.R. Parameswaran, M.H. Chou, M.M. Fejer, Spectral phase correlator for coded waveform recognition using second harmonic generation, Ultrafast Phenomena XIII, Springer, Berlin, 2000, in press.